THE JOURNAL OF BIOLOGICAL CHEMISTRY
Vol. 279, No. 50, Issue of December 10, pp. 52630–52642, 2004
Printed in U.S.A.

Myocardial Cell Death and Regeneration during Progression of Ca

This article has been withdrawn by Sagartirtha Sarkar, Mamta Chawla-Sarkar, Kazutoshi Nishiyama, Joe G. Hollyfield, and Subha Sen. David Young and Mary E. Rayborn could not be reached. The images from 9-month-old mice in Fig. 1*A* were reused from Sarkar, S., *et al.* (2004) *J. Biol. Chem.* **279,** 20422–20434 as 1-year-old and 18-week-old mice. The withdrawing authors state that they showed the images of the heart at the recommendation of a reviewer to introduce the model. The first four lanes of the GAPDH immunoblot in Fig. 3*B* were reused in the last four lanes as well as in Figs. 3*D*, *6* (*B* and *C*), and 8*B* and Sarkar, S., *et al.* (2004) *J. Biol. Chem.* **279,** 20422–20434. Additionally, the GAPDH immunoblots in Figs. 3*D* and 6 (*B* and *C*) are the same. In Fig. 3*B*, the first two lanes of the Fas immunoblot are the same. In Fig. 6*B*, the first two lanes of the cyclin D3 immunoblot are the same. In Fig. 6*C*, the first two lanes of the Cdk1 immunoblot are the same.

The withdrawing authors do not agree that the first four lanes of the GAPDH immunoblot in Fig 3*B* were reused in the last four lanes as well as in Figs. 3*D*, 6 (*B* and *C*), and 8*B* and in Sarkar, S., *et al.* (2004) *J. Biol. Chem.* **279,** 20422–20434. The withdrawing authors state that they provided evidence that these images are different based on different densitometric scan values for each lane under question, as well as few background differences among the GAPDH lanes. Similar evidence was also presented for the GAPDH immunoblots in Figs. 3*D* and 6 (*B* and *C*). However, the Journal did not agree with the withdrawing authors' evidence. The withdrawing authors strongly disagree on any duplication between the first two lanes of the Fas immunoblot in Fig. 3*B*, the first two lanes of the cyclin D3 immunoblot in Fig. 6*B*, and the first two lanes of the Cdk1 immunoblot in Fig. 6*C*. The withdrawing authors could not produce any original autoradiograms or scans to support their claims for the publication, which is 17 years old due to closure of the laboratory for more than a decade. Therefore, due to the unavailability of the original data after so many years, the withdrawing authors decided to withdraw the manuscript. The withdrawing authors state that none of the results presented in this article were compromised and the conclusions of each experiment remain unaltered.

* T
HL2
artic
artic
with
‖ T
Card
Cleveland, OH 44195. Tel.: 216-444-2056; Fax: 216-444-3110; E-mail: sens@ccf.org.

[1] The abbreviations used are: PCD, programmed cell death; Tg, transcardiomyopathic; NF, nonfailing; TNF-α, tumor necrosis factor-α; RPA, RNase protection assays; DAPI, 4,6-diamidino-2-phenylindole; Cdk, cyclin-dependent kinases.

TABLE I
Clinical characteristics of the human heart samples used in this study

	Code	Diagnosis	Age	Sex
Nonfailing	A1	MVA[a]	52	Male
	A2	MVA	51	Female
	A3	MVA	53	Female
	A9	MVA	46	Female
	A10	MVA	52	Male
Failing	A4	DCM	52	Male
	A5	DCM	57	Female
	A7	DCM	58	Male
	A12	DCM	51	Female
	A13	DCM	47	Female

[a] MVA, motor vehicle accident.

transgenic animals during initiation (about 4 weeks of age) and transition of hypertrophy to heart failure (around 36 weeks of age). A cluster of apoptotic genes, as well as genes involved in cellular regeneration, was found to be significantly up-regulated in 36-week-old Tg mice heart samples but not those from 4-week-old mice (9). Therefore, we chose to study the molecular changes for both cardiac cell death and regeneration during initiation of cardiac hypertrophy and during the transition from hypertrophy to heart failure, the later still being an open question. To establish the relevance of our findings in murine model, we also studied some key genes in these processes (active caspase 3 for cell death and Ki-67 for cell regeneration) in human dilated cardiomyopathic (DCM) and nonfailing (NF) hearts. Our data showed that both cell death and regenerati
occur simultaneously during heart failure that is not
during onset of this disease.

EXPERIMENTAL PROCEDUR

Animals Used—All mice used in this
Harlan Sprague-Dawley (Indianapoli
formed to the "Guide for the Care
For each experiment discus
animals, both wild-type (
(4 weeks and 9 months),
four founder lines that ov
Our data represent both m
ence was observed between
studied.

Human Samples—Human D
tained from the cardiac transpla
Foundation. NF human hearts wer
suitable for transplantation but with
were victims of either motor vehicle accidents or gunshot wounds. Failing hearts were obtained from 6 transplant patients diagnosed with DCM. All heart samples were transported to the laboratory in cold cardioplegia and were snap frozen instantly for future use. Protocols for tissue procurement were approved by the Cleveland Clinic Foundation Institutional Review Board. The clinical characteristics of these heart samples are tabulated in Table I.

TUNEL Assay—DNA fragmentation was detected in left ventricular sections of 9-month-old WT and Tg mice by TUNEL staining using the APO-BRDU™ kit (BD Pharmingen, San Diego, CA). Briefly, the sections were passed through graded alcohol and labeled with bromodeoxyribonucleotide triphosphate, washed twice with phosphate-buffered saline, and labeled with bromodeoxyribonucleotide triphosphate by the terminal deoxynucleotidyl transferase enzyme for 2 h at 37 °C. After labeling, sections were washed and stained with fluorescein isothiocyanate-conjugated anti-bromodeoxyuridine monoclonal antibody for 30 min in a low-light environment. RNase was added and samples were incubated for an additional 30 min at room temperature. Slides were rinsed 3–4 times with 1× phosphate-buffered saline before being mounted with Vectrashield (Vector Laboratories Inc., Burlingame, CA). The percentage of fluorescein isothiocyanate-positive cells was analyzed by fluorescence microscopy using an excitation wavelength in the range of 450–500 nm and detection in the range of 515–565 nm (green). Negative controls included sections incubated in the absence of substrate.

RNase Protection Assay—Total RNA was isolated from WT and Tg mice hearts and human heart samples using TRIzol reagent (Invitrogen). RNase protection assays (RPAs) were done using the RiboQuant system with a multiprobe template set from BD Pharmingen. For mice, the mAPO-1, mAPO-2, mAPO-3, and mCYC-1 template sets were used for T7 polymerase directed synthesis of high specific activity [^{32}P]UTP-labeled antisense RNA probes. The probe sets contained 13 probes including two housekeeping genes, *GAPDH* and *L32*. Probes (4×10^5 cpm) were hybridized with each RNA (10 μg) sample overnight at 56 °C. RNA samples were digested with RNase A and T1, purified, and resolved on 6% denaturing polyacrylamide gels. Internal housekeeping genes were analyzed to confirm equal RNA loading. For failing and nonfailing human heart samples ($n = 5$), multiprobe template sets hAPO-1c, hAPO-2c, hAPO-3, and hCYC-1 were used for RPA, following the manufacturer's protocol.

Immunohistochemistry—Myocardial sections were stained with antibodies against Fas, Fas-associated death domain (FADD), the cleaved active form of caspase-8, -7, and -3, or the macrophage markers CD13 and CD14 (BD Pharmingen). The sections were counterstained with propidium iodide and analyzed by fluorescent microscopy (26).

Active caspase-3 (BD Pharmingen) and Ki-67 (DAKO Corp., Carpinteria, CA) proteins were used for confocal microscopic analysis along with α-actinin antibody (Sigma) on myocardial sections with nuclear counterstaining agent (DAPI) by using an SP2 confocal laser scanning microscope (Leica, Heidelberg, Germany), equipped with 40, 60, and 100× infinity-adjusted
nmersion objectives and triple channel photodetectors. Both m
d Tg) and human (NF and DCM) ventricular sections we
cal studies with active caspase-3 and Ki-67 (detect
tinin (detected in red; $n = 5$). Each data set
icroscope was processed with software
operating system, and used to co
omputer-averaged assem-
ibodies against cyclin B1
osphohistone H3 (Cell
d on 36-week-old Tg

re lysed in 1× lysis buffer (50
, 10% glycerol, 1 mM EDTA, 250 mM
mM phenylmethylsulfonyl fluoride, 10
l leupeptin, and 10 μg/ml pepstatin) and
0 μg of protein were fractionated by 12% SDS-
sferred to polyvinylidene difluoride membranes. The
were subsequently incubated with monoclonal antibody to
12, Fas, tumor necrosis factor (TNF)-α RI and RII (Santa Cruz
echnology, Inc.), polyclonal antibody to active caspase-3 (BD Pharmingen), caspase-8 (Stressgen Biotechnologies Corp., Victoria, BC, Canada), Bcl-X_L (Transduction Laboratories, San Diego, CA), or polyclonal antibody to cyclin A, B_1, or B_2 (Santa Cruz Biotechnologies) followed by incubation with horseradish peroxidase-conjugated secondary antibodies (Pierce). Immunoreactive bands were visualized using enhanced chemiluminescence (PerkinElmer Life Sciences). Equal protein loading was confirmed by staining the gel with Coomassie Blue and probing with GAPDH antibody (Novus Biologicals Inc., Littleton, CO).

Caspase Activity Assay—The activity of caspase-3, -8, and -9 was measured using a commercially available caspase assay kit (Clontech). Briefly, tissues were washed twice with cold phosphate-buffered saline and lysed on ice in 1× lysis buffer provided by the company. Tissue lysates were centrifuged at 10,000 × g for 10 min, and the total protein concentration was estimated using a protein assay reagent (Bio-Rad). The assay was performed in triplicate in 96-well plates. For each caspase-3 assay, 20 μg of protein extract, 200 μl of 1× Hepes buffer, and 5 μl of Ac-DEVD-AFC (a fluorogenic substrate) were mixed and incubated at 37 °C for 1 h. As a control, cell lysates or substrate alone were incubated in parallel. Enzymatic hydrolysis of caspase-3 was measured by AMC liberation from Ac-DEVD-AFC at 380/460 nm using a spectrofluorometer. Relative fluorescence of substrate control was subtracted as background emission. Activity of caspase-8 and -9 was measured using Ac-IETD-AFC and Ac-LEHD-AMC substrates, as described for the caspase-3 assay.

Cyclin-dependent Kinase Activity Assay—Six hundred micrograms of tissue lysate from Tg and WT hearts lysed in buffer (50 mM Hepes, pH 7.0, 150 mM sodium chloride, 10% glycerol, 0.1% Tween 20, protease inhibitor mixture (Calbiochem, San Diego, CA), 0.5 mM sodium pyrophosphate, 0.1 mM sodium orthovanadate, and 5 mM sodium fluoride) were immunoprecipitated with polyclonal antibody to Cdc2, Cdk2, or Cdk4 (Santa Cruz Biotechnologies) for 2 h at 4 °C. The protein A-Sepharose beads containing the immunocomplexes were incubated with 25 μl of kinase buffer, 2 μg of histone H1 (as substrate for Cdk2) or 0.5 μg of retinoblastoma pRb (as Cdk4 substrate, Santa Cruz Biotechnology Inc.) and 1 μl of 3000 Ci/mM [γ-^{32}P]ATP (PerkinElmer Life Sciences) for

30 min at 30 °C. The samples were subjected to 10% SDS-PAGE, and the gel was exposed to autoradiographic film. To assess the background kinase activity, all the samples were immunoprecipitated with preimmune rabbit IgG and were run parallel on the gel. Background kinase activity was subtracted (27).

Isolation of Cardiac Myocytes from Hearts of WT and Tg Mice Overexpressing Myotrophin—As described previously (28), hearts were taken out from heparin-injected mice and cannulated via aorta (n = 6). Hearts were perfused with perfusion buffer (glucose, 1 g; $NaHCO_3$, 0.58 g; and pyruvic acid, 0.27 g, pH 7.3) with 95% O_2 and 5% CO_2 on a Langendorff apparatus. After perfusing the heart for 10 min in EGTA-supplemented perfusion buffer, hearts were digested using collagenase (2 mg/ml) for 28 min, with gradual enhancement of $CaCl_2$. After 28 min of digestion with collagenase, the heart was taken out and incubated in a diluted collagenase solution for 10 min in a shaking water bath at 37 °C. The ventricles were separated from the atria, triturated for 30 s, and subsequently filtered through cheesecloth. The filtrate was centrifuged at 400 rpm for 2 min, the supernatant was removed, and the pellet was resuspended in 4% bovine serum albumin solution and observed under a phase-contrast microscope. Preparations with 80–85% beating rod-shaped cells were used for experimental purposes.

Isolation of Nuclear Protein from the Isolated Myocytes—Nuclear protein was prepared using NE-PER nuclear and cytoplasmic extraction reagents (Pierce), using the manufacturer's protocol. Both cytoplasmic and nuclear fractions were collected, the amount of protein was measured using standard techniques, and Western blots were performed as described earlier with primary antibodies. Twenty micrograms of nuclear protein was used to detect proteins using monoclonal antibodies to poly(ADP-ribose) polymerase (PARP) (Biomol, Plymouth Meeting, PA), pCNA (Santa Cruz Biotechnologies), and phosphohistone H3 (Cell Signaling Technology, Beverly, MA). Twenty micrograms of cytoplasmic proteins was used to detect c-*kit* and Sca-1 (R&D Systems, Minneapolis, MN) using the respective antibodies. These blots were probed with GAPDH antibody as a loading control.

Statistical Analysis—Each experiment was repeated [illegible] times. Results were expressed as mean ± S.E. Data [illegible] two-way analysis of variance, and differences [illegible] determined by the least-square means test. [illegible] cance was evaluated using the analysis [illegible] 0.05 was considered significant.

Detection of Cell [illegible] WT Mice

Cell death (apoptosis) was [illegible] (n = 6) from 4-week-old and 9-month-old [illegible] significant hypertrophy (heart weight:body [illegible] 0.4 ± 0.4 compared with 4.7 ± 0.1 in WT) [illegible] matched WT mice by TUNEL staining. In 9-month-old [illegible] hearts, only 5–8 nuclei per 10^5 cells were TUNEL positive (Fig. 1*B*). Apoptotic nuclei were absent in young (4-week-old) transgenic heart sections. This value was markedly increased in ventricular sections of failing hearts from 9-month-old Tg mice in which TUNEL-positive cells appeared to be distributed toward the distal end of the myocardium. The number of TUNEL-positive nuclei varied between 85 and 185 per 10^5 cells among different heart sections from 9-month-old Tg mice (n = 12). There were an average of 130 TUNEL-positive nuclei per 10^5 cells (Fig. 1*B*), resulting in an almost 12-fold increase in the number of apoptotic cells in failing hearts compared with nonfailing hearts of the same age group.

FIG. 1. *A*, phenotype of the heart in 9-month-old Tg mice and age-matched WT controls. *Panel 1*, heart size in WT and Tg mice; *panel 2* shows the increased number of nuclei as well as a typical myocyte disarray in the Tg heart section (scale bar = 10 μm). *B*, apoptosis was analyzed by TUNEL staining of 4-week and 9-month-old Tg and WT mice ventricular sections, using a standard APO-BRDU™ kit (BD Pharmingen). TUNEL-positive nuclei were observed only in 9-month-old Tg mice but were absent in the age-matched WT mice. The number of TUNEL-positive cells varied between 75 and 185 per 10^5 cells among different heart sections of 9-month-old Tg mice (n = 12). TUNEL-positive cells were absent in 4-week-old Tg heart samples (scale bar = 20 μm).

Comparison of Apoptotic Gene Expression between Initiation and Progression of Disease Process

RNA Profiling: by RNase Protection Assay—RPA studies were performed using RNA from 4-week-old and 9-month-old WT and Tg mouse hearts (n = 5) with mouse multiprobes mAPO1, mAPO2, and mAPO3 (BD Biosciences Pharmingen; Fig. 2). Several apoptosis-regulating genes were up-regulated in the 9-month-old Tg hearts compared with either the age-matched WT or 4-week-old Tg hearts. Transcript levels of genes involved in the death receptor pathway were analyzed using a mAPO1 probe set (caspase-8, *Fas*, *FADD*, Fas-associated phosphatase, Fas-associated factor, TNF-α-related apoptosis-inducing ligand, *TNF-α Rp55*, TNF-α receptor-1-associated death domain protein, *RIP*, *L32*, and glyceraldehyde-3-phosphate dehydrogenase). Four genes were up-regulated in 9-month-old Tg mice compared with the age-matched wild-type controls or 4-week-old Tg mice: *Fas* >5-fold, *FADD* >4-fold, TNF-related

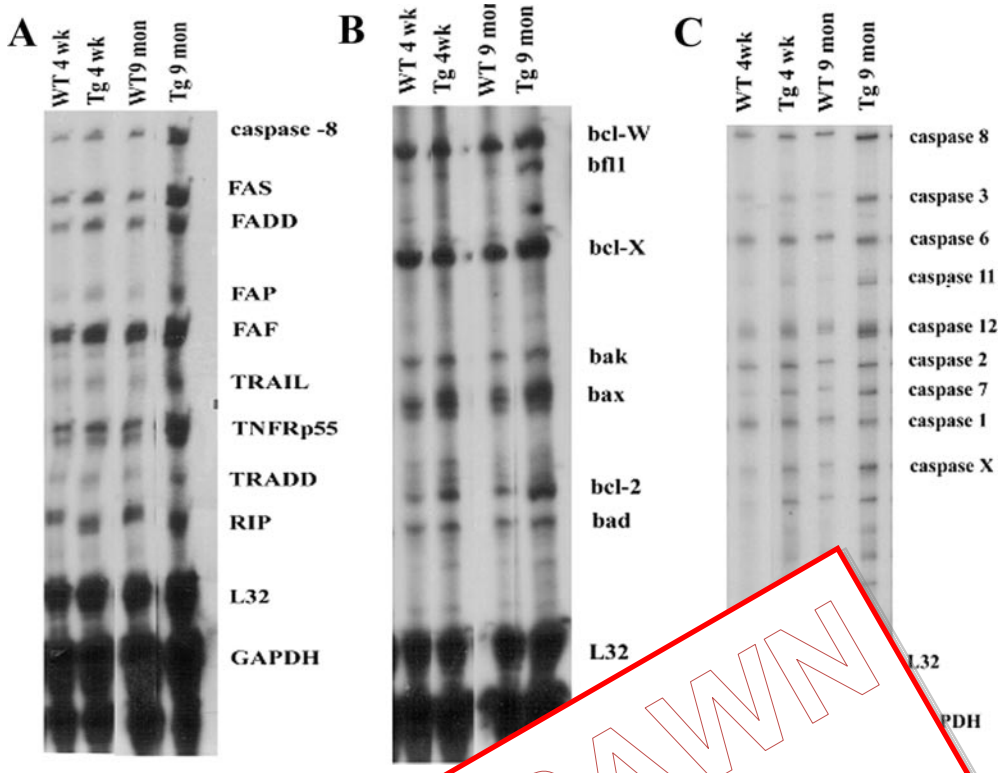

FIG. 2. **Changes in expression of apoptotic genes in tra** ssion was analyzed using RPA multiprobes mApo1 (*panel A*), mApo2 (*panel B*), and samples of 4-week-old and 9-month-old Tg mice and age-matched WT controls. *4W* d WT; and *9Tg*, 9-month-old Tg. Maximum up-regulation of caspase-8, *Fas*, *FADD*, *T* ed in 9 Tg mice compared with either 4 Tg or the WT controls. The figure is represe

apoptosis-inducing ligand >2-fo ax protein in failing hearts, whereas Bcl2 was >4-fold (Fig. 2*A*, $p < 0.01$) d by almost 5-fold in 9-month-old transgenic hearts , compared with either age-matched WT or 4-week-old mice. Induced expression of Bax protein was observed by Western blot analysis during the initiation phase of hypertrophy (4-week-old Tg compared with age-matched WT), although induced Bax protein was not observed in these hearts by immunohistological staining.

Changes in the expr family (mAPO2) were Tg mice and WT contr scripts were up-regulate th- old Tg mice compared wit ce (Fig. 2*B*, $p < 0.01$). *Bcl2* transcri by 2-fold in failing heart samples. No sign e was observed in levels of *Bak* and *Bad* transcri initiation and transition phases of the disease.

Significant up-regulation of the initiator and effector caspases, namely, caspase-3, -7, -8, and -12, were observed in failing hearts compared with normal or 4-week-old hearts during initiation of hypertrophy (Fig. 2*C*). No significant differences were observed in caspase-6, -2, and -1 transcripts between Tg and WT hearts. On the other hand, a >2-fold increase in caspase-X and -11 transcripts was observed in failing hearts only. *L32* and *GAPDH* genes were used as internal loading controls (Fig. 2, *A–C*).

Changes in Protein Expression: Immunoblot and Immunohistochemistry—(i) Immunohistological data showed increased expression of Fas and FADD in left ventricle sections of 9-month-old Tg heart compared with 4-week-old Tg mice or age-matched WT ($n = 5$; Fig. 3*A*). Immunoblot analyses detected a 2.5-fold increase in FAS and TNF-α expression and a 2-fold increase in TNF-α RI in 9-month-old Tg compared with WT mice (Fig. 3*B*). No change was observed during the initiation phase of hypertrophy in 4-week-old Tg mice, compared with age-matched WT for Fas, although a slight induction in TNF-α protein was observed in 4-week-old Tg.

(ii) Bcl2 and Bax proteins were also up-regulated in failing Tg hearts compared with nonfailing hearts (Fig. 3, *C* and *D*). Immunohistological as well as immunoblot data showed a 2.5-

(iii) Fig. 4*A* shows immunohistochemistry using antibodies against active fragments of caspase-3, -7, and -8 ($n = 5$). Data showed no difference in expression levels of the caspases between 4-week-old WT and Tg. However, a significant increase in expression of active caspases was observed in 9-month-old Tg mice hearts compared with either age-matched WT or 4-week-old Tg mice. Cleavage of caspase-3 and -8 was further confirmed by immunoblot analyses. Active fragments (p17 and p32) were detected in the failing hearts (9-month-old Tg) only but not in nonfailing hearts from WT or 4-week-old Tg mice (Fig. 4*B*).

(iv) Induction of infiltrating macrophages, CD13 and CD14, was detected by immunohistological staining in failing heart sections only (9-month-old Tg; Fig. 4*C*, $n = 5$). Infiltration of macrophages was not detected in any of the nonfailing heart samples (9-month-old WT or 4-week-old Tg). High numbers of infiltrating macrophages in failing hearts may be involved in phagocytosis of dead cells in the tissue.

Biochemical Analysis of Activity of Caspases in Cellular Extracts of Tg and WT Hearts—Because immunoblot analyses confirmed the presence of active caspases in the Tg hearts, caspase activity was measured in hearts from both Tg and WT mice using specific fluorogenic substrates (ApoAlert; Clontech, Palo Alto, CA) for caspase-3, -8, and -9. No difference was observed in caspase-3 activity levels between heart samples of 4-week-old WT and Tg mice. A slight but nonsignificant in-

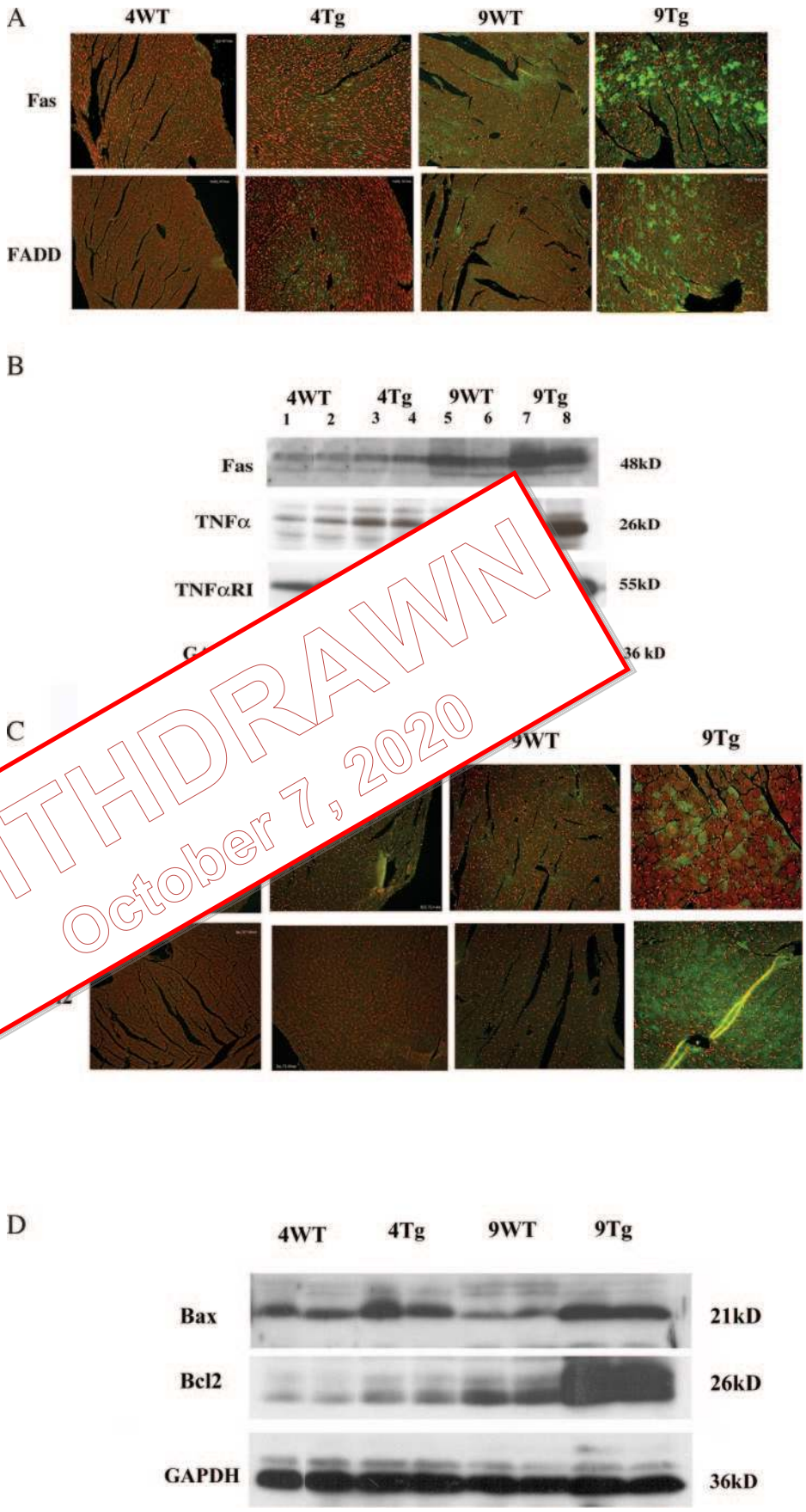

FIG. 3. **Detection of apoptotic proteins in Tg samples (n = 5) by immunohistochemistry and immunoblot analysis during initiation (4 weeks) as well as transition from hypertrophy to heart failure (9 months).** *A*, immunohistology using FADD and Fas antibody to heart sections of WT and Tg mice (scale bar = 10 μm). Induction of FADD and Fas protein was observed in 9-month-old Tg heart sections. *B*, immunoblot analysis using FAS, TNF-α, and the TNF-α receptors (TNF-α RI and TNF-α RII) shows significant changes in expression of these proteins in 9-month-old Tg samples. *C*, immunohistology using Bax and Bcl2 antibody to heart sections of 4-week-old and 9-month and Tg mice (scale bar = 10 icant expression of Bax was observed in 9-month *D*, immunoblot analysis Bcl2 antibodies to WT and tracts from 4-week-old and mice. Both Bax and Bcl2 pro significantly up-regulated in 9-m Tg heart samples compared with old Tg or WT samples.

crease in caspase activity was also detected in 4-week-old Tg hearts compared with age-matched wild-type hearts, especially for caspase-8 and -9. Activity of the executor caspase, caspase-3 was increased 92.5% in hearts from 9-month-old Tg mice, whereas the activities of the initiator caspases, caspase-8 and -9, were increased by 59 and 79%, respectively, compared with

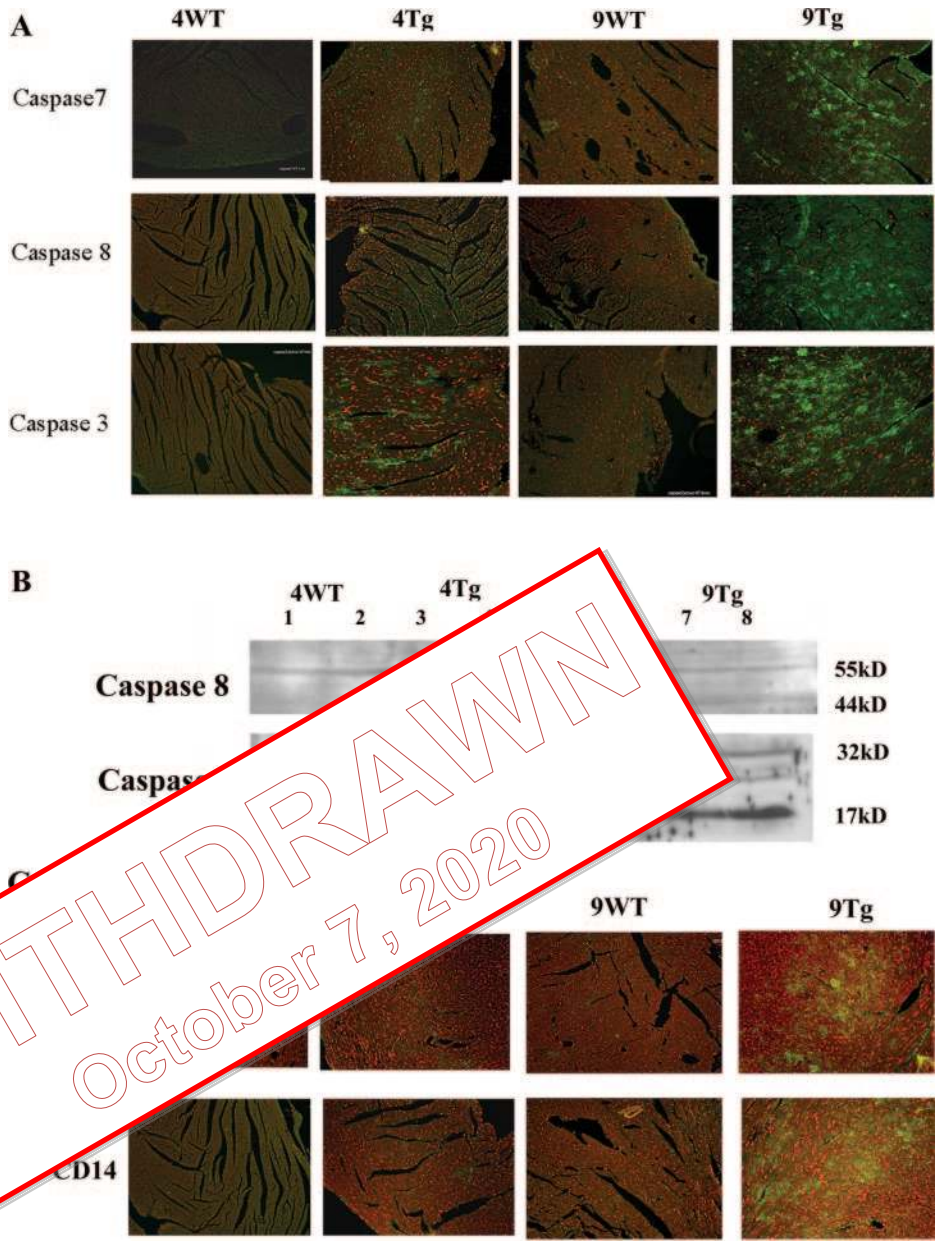

FIG. 4. **Comparative analysis of expression of several upstream and downstream caspase proteins in 4-week-old and 9-month-old Tg mice hearts (n = 5) compared with age-matched WT by immunohistochemistry and immunoblot analyses.** *A*, immunohistology using caspase-3, -7, and -8 antibodies to heart sections from WT and Tg mice (scale bar = 10 μm). Significant induction for these caspases was observed in 9-month-old Tg heart samples compared with the age-matched WT or 4-week-old Tg ones. The antibodies used to detect caspases were generated against their active fragments. *B*, immunoblot analysis using antibodies against caspase-3 and -8 in failing and nonfailing heart samples. Cleaved active fragments of both caspase 8 (44 kDa) and -3 (17 kDa) were observed only in 9-month-old Tg mice during transition from hypertrophy to heart failure. The active fragments were absent in either 4-week-old Tg or the WT samples. The blot represents results of five independent experiments. *C*, immunodetection of infiltrating macrophages in tissue samples of WT and Tg heart sections of 4-week-old and 9-month-old mice (scale bar = 10 μm). An increase in the concentration of infiltrating macrophages was observed in failing heart samples using antibodies specific for CD13 and CD14 marker proteins. Infiltration
macrophages in 9-month-old Tg su
the possibility of increased ph
of dead cells in the tissue d
sition of hypertrophy
CD13 and CD14 marke
undetected in age-matched
tions as well as 4-week-old

age-matched WT samples or 4-week-old Tg mice hearts (n = 5; $p < 0.01$; Fig. 5).

Consequence of Long-standing Hypertrophy on the Cell Cycle Regulator Genes in Mice

Despite significant cell death in Tg mice hearts, the heart weight:body weight ratio was >12, implicating either increased cell division (mitosis), cell enlargement, or both. To analyze how the transition from hypertrophy to heart failure in 9-month-old Tg hearts affects the expression of cell cycle regulatory genes, both RPA and immunoblot analyses were performed.

RPA Analysis Using Cyclin Multiprobes—RPA studies using the mouse mCdk3b multiprobe of cell cycle regulatory genes showed significant up-regulation of different cyclin transcripts in the hearts of Tg mice. Maximum induction was observed for *cyclin B1* and *B2* transcripts (~4-fold) in failing heart. The *cyclin D* family (*D1*, *D2*, and *D3*) was up-regulated by 2-fold, *cyclin A2* by 3-fold, and *cyclin C* by 1.2-fold in hearts of 9-month-old Tg mice, compared with 9-month-old WT (n = 5; Fig. 6*A*). Some of the cyclin genes (*cyclin C*, *D2*, and *D3*) were induced in the 4-week-old Tg heart samples (although to a much lesser degree than 9-month-old Tg) when compared with age-matched WT samples.

Immunoblot Analyses—Changes in the cell cycle regulator genes (*cyclin A*, *B1*, *D1*, and *D3*) between WT and Tg heart samples were further confirmed at the protein level. Western blot analysis showed maximum up-regulation of *cyclin A* as >4-fold, *cyclin B1* as >3-fold, *cyclin D1* as >5-fold, and *cyclin D3* as ≥2-fold (n = 5; Fig. 6*B*) in 9-month-old Tg animals compared with age-matched WT or 4-week-old Tg hearts. Some induction (although nonsignficant) in the protein level of these cyclins was also observed in Tg mice at as early as 4 weeks, during initiation of hypertrophy, when compared with their age-matched WT.

Changes in Cyclin-dependent Kinases—Cdks regulate the action of the cyclin genes. Cdk-1 (Cdc2), Cdk-2, and Cdk-4 bind to *cyclin A*, *B*, and *D*, respectively. Once it was determined that cyclin genes were up-regulated in hypertrophic heart, immunoblot analyses were done to analyze the protein expression of

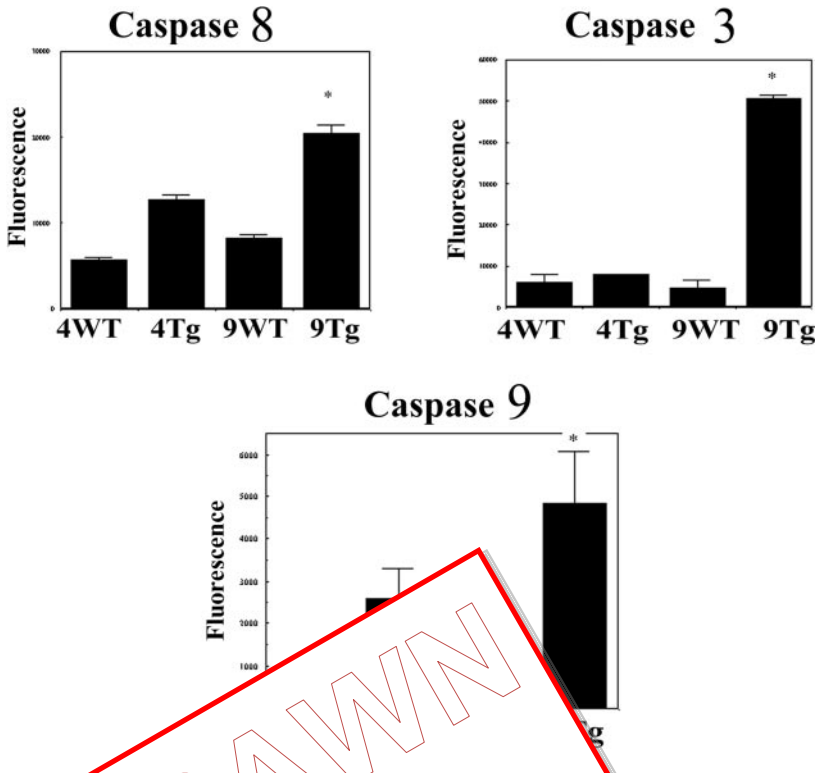

FIG. 5. **Increase in caspase activity correlates with considerable cell death in Tg mice.** Activity of the cysteine proteases (caspase-3, -8, and -9) was measured using the ApoAlert kit (Clontech). A significant increase ($n = 5$; $p < 0.01$) in the activity of caspase-3, -8, and -9 (92, 59, and 79%, respectively) was observed in failing hypertrophic hearts compared with the age-matched WT controls. A nonsignificant increase in activity of caspase-8 and -9 (15%) was also detected in Tg animals as early as 4 weeks of age compared with 4-week-old WT.

different Cdks. However, only Cdk-1 (not Cdk-2 and -4 a significant change in protein expression levels i Tg animals, compared with either age-matc old Tg (Fig. 6*C*).

However, because kinase activit cycle, *in vitro* kinase assays w in kinase activity during heart failure. The ki significantly elevated ing animals. Maximum served for Cdk-2 (about 4 ity was documented for 9-month-old Tg mice (Fig. 6 kinase activity was documen matched WT.

and the appearance of an protein in cardiomyocytes of cument the occurrence of PCD in ailure.

ocyte nuclei stained positive for the Ki-67 same myocardial sections of failing mouse heart *panel A–D*). No Ki-67-positive myocytes were docued in myocardial sections of age-matched WT or in -week-old Tg mice. The nuclei in these sections were counterstained with DAPI (*blue*). Ki-67 immunostaining (*green*) was observed in nuclei of some myocytes, whereas the cytoplasm was labeled with α-actinin (*red*) antibody. The Ki-67-positive nuclei in myocytes were few in the failing heart sections (the number of Ki-67-positive myocytes in 9-month-old Tg hearts was 23 ± 0.89 in 2253 ± 53.3 myocytes examined, $n = 5$; $p < 0.01$).

Significant induction of several other cell cycle marker proteins by Western blot was observed in isolated cardiac myocytes from 9-month-old Tg mice compared with either age-matched WT or 4-week-old Tg or WT mice (Fig. 8*B*). Proliferation of cell nuclear antigen (*pCNA*, *panel 1*) and phosphohistone H1 (Ser-10) protein (*panel 2*) showed maximum induction in myocytes during heart failure (9-month-old Tg) compared with either age-matched WT mice or during the initiation phase of hypertrophy (≥5-fold, $n = 5$, $p < 0.01$). An almost 2-fold induction for c-*kit* (*panel 3*) and Sca-1 (*panel 4*) proteins was also observed in 9-month-old Tg myocytes compared with myocytes isolated from nonfailing heart samples (Fig. 8*B*). Furthermore, we colocalized overexpression of cyclin B1 protein and phosphohistone H3 in the myocardial sections from 9-month-old Tg mice. We also confirmed the presence of these cell cycle marker proteins in myocytes that stained positive with α-actinin, as shown in Fig. 8*C*. Induction of these proteins in 9-month-old Tg myocytes clearly indicates that the myocytes are beginning to undergo or actually undergoing cell division during the transition of hypertrophy to heart failure, a state that is not documented during onset of hypertrophy or during progression of this disease process.

Cell Death and Regeneration Occurs in Myocytes of Failing Murine Hearts

Because we had already shown that apoptosis and cellular regeneration occur during the transition of hypertrophy to heart failure, our next goal was to confirm whether cell death and regeneration occurs in cardiac myocytes in the failing heart. As shown in Fig. 7*A* many myocytes in 9-month-old Tg heart sections detected by α-actinin (*red*) were also positive for active caspase-3 protein (*green*; *panel b*). WT sections (*panel a*) did not show the presence of active caspase 3 proteins in myocytes stained with α-actinin. The subcellular localization of active caspase-3 and α-actinin varied between each other, whereas both of them are present in the cytoplasm of the myocytes. Analysis of confocal microscopic studies involved myocardial sections from five different WT and Tg mice.

Nuclear protein isolated from myocytes of WT and Tg mice hearts during initiation of hypertrophy as well as transition from hypertrophy to heart failure (4-week-old and 9-month-old mice) showed intact PARP protein (116 kDa) in protein samples of both 4-week-old WT and Tg as well as 9-month-old WT myocytes. Cleavage of the PARP protein (89 kDa) was observed in 9-month-old Tg myocytes ($n = 5$; Fig. 7*B*). The induced

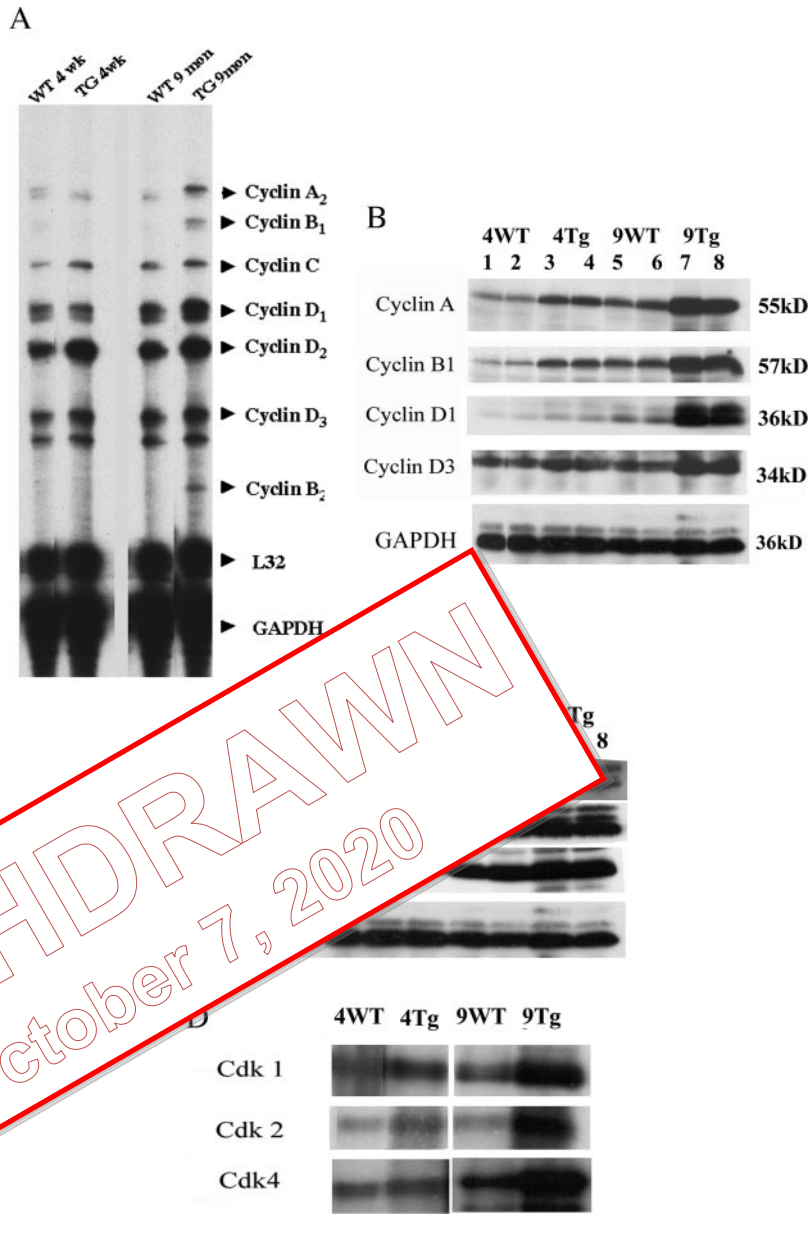

FIG. 6. **Changes in expression of cyclin gene transcripts and proteins during the initiation phase of hypertrophy and the transition from hypertrophy to heart failure in Tg mice compared with age-matched WT mice ($n = 5$).** *A*, RPA profile of the WT and Tg mouse hearts from different age groups, using mCyc multiprobe, shows age-dependent induction of cyclin genes. Many of these cyclin transcripts were turned on considerably in 9-month-old Tg mice compared with 9-month-old WT. A slight increase in some of the cyclin transcripts was also observed in 4-week-old Tg compared with age-matched WT mice. The picture represents results from five independent experiments. *B*, immunoblot analysis showed significant induction of the cyclin proteins (cyclin A, B1, D1, and D3) in 9-month-old Tg compared with either age-matched WT or 4-week-old Tg mice. *C*, changes in kinase activity of Cdk1, Cdk2, and Cdk4 because of long-standing hypertrophy were analyzed by Western blots using antibodies to Cdk1, Cdk2, and Cdk3 in 4-week-old and 9-month-old Tg and WT mice heart samples. Western blot analysis showed no significant change in the protein level of these Cdks between WT and Tg heart samples of any age, either during the initiation or transition phase of hypertrophy to heart failure. *D*, *in vitro* kinase assays were performed to analyze kinase activ of the cell cycle regulator kinases tically significant up-regulati Cdk-2, and Cdk-4 activity failing hearts (9-mont with either age-matched old Tg mice.

Changes in Apoptotic and Cell Cycle Regulator Genes in DCM Human Hearts

RPA Analysis—Several apoptotic genes both upstream and downstream and cell cycle regulator genes (similar to the murine heart failure model) were found to be up-regulated in DCM hearts compared with NF samples ($n = 5$). Among the apoptotic genes, *FAS*, *TRAIL*, several death receptors (*DR3* and *DR4*), *BCL-X*, *BAX*, and *BCL2* were significantly up-regulated in DCM hearts compared with nonfailing samples (Fig. 9*A*, $p < 0.05$). Among several caspase transcripts, caspase 3 and caspase 9 were maximally up-regulated in failing hearts similar to what was observed in the myotrophin-overexpressed Tg mouse model. Cell cycle regulator genes like *cyclin A*, *cyclin C*, and *cyclin D* were also turned on in DCM hearts (Fig. 9*A*, $p < 0.01$).

Immunohistology and Confocal Microscopy—To confirm our observation that apoptosis and cell regeneration occurs simultaneously in cardiomyocytes during heart failure in the Tg mice model, confocal microscopy studies were performed with active caspase 3 (marker for apoptosis) and Ki-67 (marker for cell regeneration) on sections of DCM and nonfailing heart samples ($n = 5$). α-Actinin antibody was used to identify cardiomyocytes in these heart sections. Our results clearly show that active caspase 3 protein was found to be significantly up-regulated in failing cardiomyocytes (positive for α-actinin) of DCM heart sections compared with nonfailing sections. 1.2% of Ki-67 positive cardiomyocyte nuclei were also observed in DCM heart sections, whereas no Ki-67 positive myocytes was found in nonfailing sections (Fig. 9*B*). Induced active caspase 3 and presence of Ki-67 positive nuclei in myocytes of DCM hearts corroborates our claim that apoptosis and cell regeneration occur simultaneously during heart failure only, as seen in the myotrophin overexpressed Tg mouse model that closely mimics human heart failure.

DISCUSSION

In this study, we have demonstrated a prevalence of DNA damage in hearts from 9-month-old Tg mice during the transition from long standing hypertrophy to heart failure, compared with the initiation phase, despite the presence of significant hypertrophy. We have also shown the induction of the cell regenerative machinery, especially in cardiac myocytes of the failing hearts. Importantly, human DCM heart samples also show similar changes in several genes for apoptosis and cell

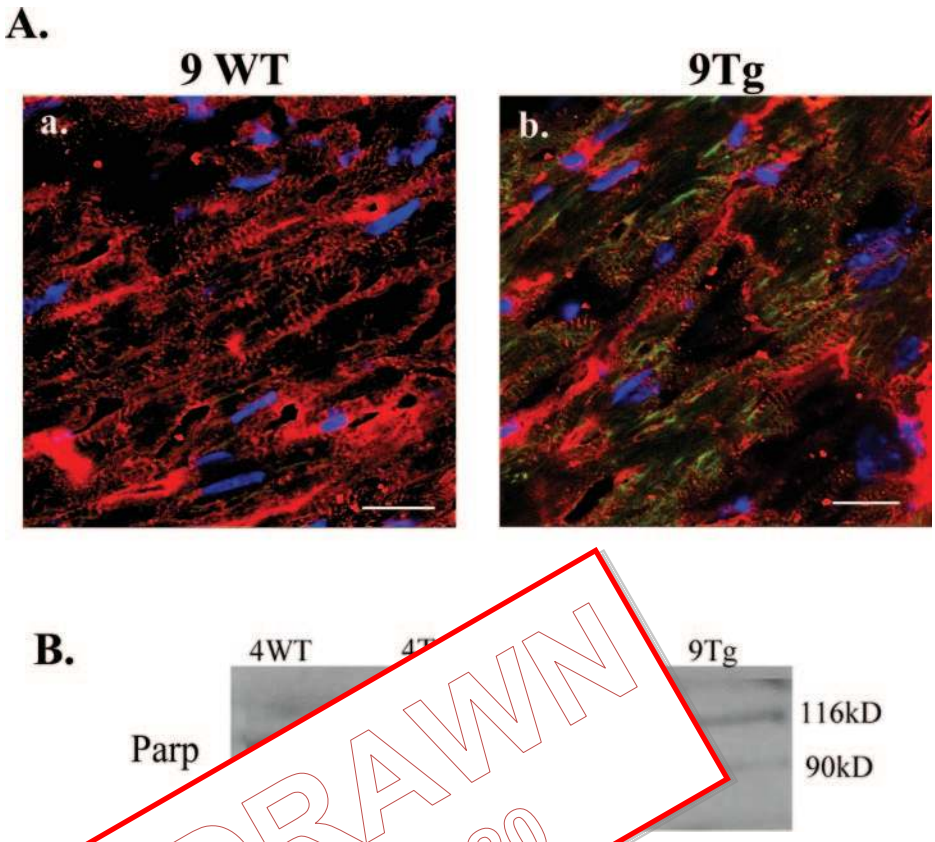

FIG. 7. *A*, confocal microscopic analysis of 9-month-old WT and Tg mice heart shows the presence of active caspase-3 (*green*) and α-actinin (*red*) immunoreactivity in Tg heart sections (*scale bar* = 20 μm). *Panel a*, 9-month-old WT heart sections showed little or no caspase-3 immunoreactivity, but were stained positive for α-actinin antibody (*red*). *Panel b*, age-matched Tg sections show the presence of active caspase 3 protein in cells positive for α-actinin (*red*). The nuclei are stained with DAPI (*blue*). *B*, Western blot analysis using anti-PARP antibody to the nuclear protein isolated from myocytes from WT and Tg mice hearts. Myocytes were isolated from 4-week-old and 9-month-old WT and Tg mice hearts ($n = 5$). Nuclear protein, from these cells was isolated as described earlier. The blot shows a cleaved PARP fragment of 89 kDa, in the 9-month-old Tg heart samples only during the transition from hypertrophy to heart failure. The cleaved product was absent in all nonfailing myocytes. The blot represents results of five independent experiments.

regeneration, compared with NF heart
mouse model (which specifically ove
the heart, develops hypertrophy
and gradually progresses t
age) convincingly sugg
place simultaneously
heart failure. In this m
nuclei were mostly localiz
left ventricle. In addition,
trated in areas where inters
In left ventricular hypertroph
the free walls of the left vent
positive nuclei were observed i
share similarities with data from the pathological analysis conducted on spontaneously hypertensive rats, in which left ventricular dysfunction was accompanied by increased cardiac apoptosis that was more frequent in free walls than in the septal region of the left ventricle (10). The number of apoptotic cells reported by these investigators and others (11) was similar to our findings.

Because it is difficult to discriminate between the individual contributions of apoptosis and necrosis during transition from hypertrophy to heart failure, quantification of the expression of different genes involved in the apoptotic pathway provides a good index of the probability that a cell will undergo apoptosis. We observed changes in some of the key apoptotic genes at the level of transcription and translation during the transition to heart failure. This result not only confirms our claim that PCD is active in this end stage of the disease process, but also implicates the probable death signal pathway in failing hearts.

Our data show that PCD or apoptosis proceeds through the classical pathway involving the upstream activators *TNF-α* or *Fas*. Significant up-regulation of adaptor molecules such as *Fas* or *TNF-α* was observed in the failing heart samples compared with the WT samples. The receptor molecules and the corresponding death domains were also induced, as well as the effector caspases (caspase-3 and -7). was observed in 9-month-old Tg hearts, cleaved product was absent in the nonfailing es (Fig. 4*B*). Caspase activity was significantly or caspase-9, -8, and -3 in failing hearts (Fig. 5). Although PCD was confirmed and possible apoptotic pathways were determined for the transition from hypertrophy to heart failure in this Tg mouse model, we could not determine exactly when this process is initiated in a hypertrophic heart. Our studies point toward the fact that PCD does not begin with the onset of hypertrophy but rather is more predominant as the hypertrophic heart progresses toward failure. It was also shown, by confocal microscopy, that active caspase-3 was present in the cytoplasm of myocytes of failing hearts (Fig. 7*A*). A cleaved product of the PARP protein (89 kDa) was also detected in myocytes of failing heart samples (Fig. 7*B*). The observed increase in caspase-3 activity, a key intermediate in the activation of apoptosis in many cell types (12) (including myocytes) (13), as well as its cleavage in the failing heart, is consistent with the conclusion that apoptosis is prevalent in the remote myocardium, especially in myocytes, during transition from hypertrophy to heart failure.

Apoptosis is initiated by the withdrawal of specific factors, and the addition of other relevant factors may prevent cell death. Certain oncogenes modulate apoptosis; *Bcl2* expression has been reported to inhibit apoptosis (14), whereas p53 (15) and c-*myc* protein (16) may induce its development. We have also observed a significant increase in expression of c-*myc* and p53 protein in the failing heart samples.[2] Some earlier reports have examined changes in the pro-apoptotic gene *Bax* and the anti-apoptotic gene *Bcl2*. In failing human hearts, Olivetti *et al.* (5) showed enhanced expression of *BCL2* in decompensated hearts compared with normal hearts, but the expression of Bax

[2] S. Sarkar, M. Chawla-Sarkar, D. Young, K. Nishiyama, M. E. Rayborn, J. G. Hollyfield, and S. Sen, unpublished data.

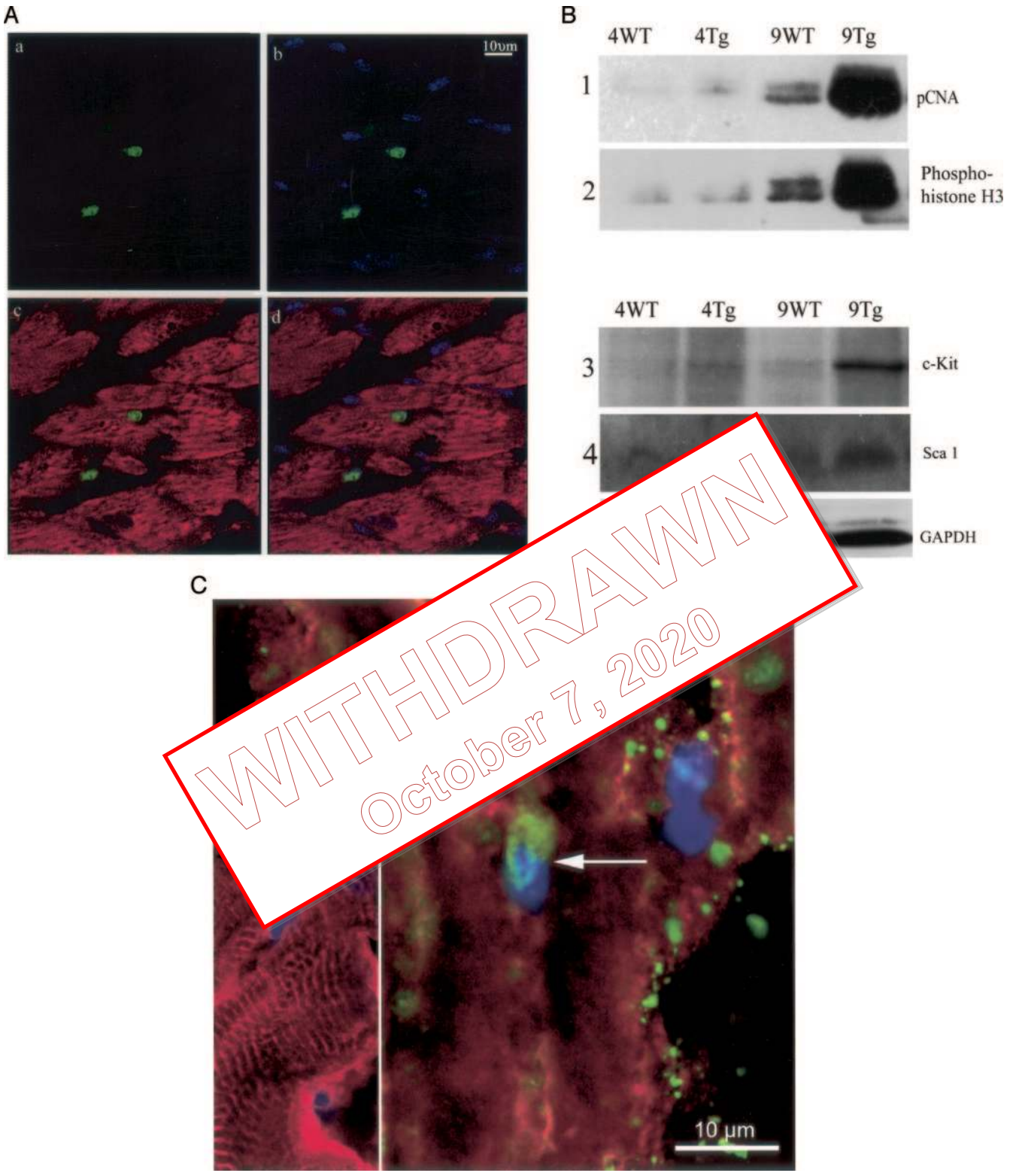

FIG. 8. *A*, confocal microscopic analysis of transgenic mice heart sections shows triple staining for Ki-67, α-actinin, and DAPI. Ki-67 positive nuclei were observed in myocytes of 9-month-old Tg mice ventricular sections only. Ki-67 positive nuclei were absent in myocytes from 4-week-old Tg mice during the initiation phase of hypertrophy. *Panel a*, immunohistochemistry for Ki-67 (*green*); *panel b*, double staining for Ki-67 (*green*) and DAPI (*blue*); *panel c*, double staining for α-actinin (*red*) and Ki-67 (*green*); *panel d*, triple staining for α-actinin (*red*), Ki-67 (*green*), and DAPI (*blue*). Some of the nuclei, but not all, present in the scanned area were positive for Ki-67-immunoreactivity (0.08%). None of the myocytes in 9-month-old WT heart sections stained positive for the Ki-67 antibody. Magnification is the same among panels of Fig. 8*A* (*scale bar* = 30 μm). *B*, Western blot analysis of several cell-regeneration marker proteins in myocytes isolated from hearts from 4-week-old and 9-month-old WT and Tg mice ($n = 5$). Nuclear protein from WT and Tg myocytes from different age groups shows significant induction of pCNA (panel 1) phosphohistone H3 (Ser-10) proteins (*panel 2*) in failing hearts of 9-month-old Tg compared with either 4 Tg or 9 WT samples. Induction of phosphohistone H3 in isolated myocytes of failing hearts indirectly confirms that some myocytes are undergoing cell division in failing hearts. Significant induction of c-*kit* (*panel 3*) and Sca-1 (*panel 4*) protein levels detected in the cytoplasmic fraction of myocytes isolated from failing heart samples compared with 9 WT or 4 Tg. GAPDH antibody was used as a loading control. The picture represents results from five independent experiments. *C*, confocal microscopic analysis of 9-month-old transgenic mice heart sections showing triple staining for cyclin B1 (*red*), phosphohistone H3 (*green*), and DAPI (*blue*). Cells overexpressing cyclin B1 also found positive for phosphohistone H3. Phosphohistone H3-positive nuclei were observed in myocytes (actinin positive, shown in inset) of similar sections.

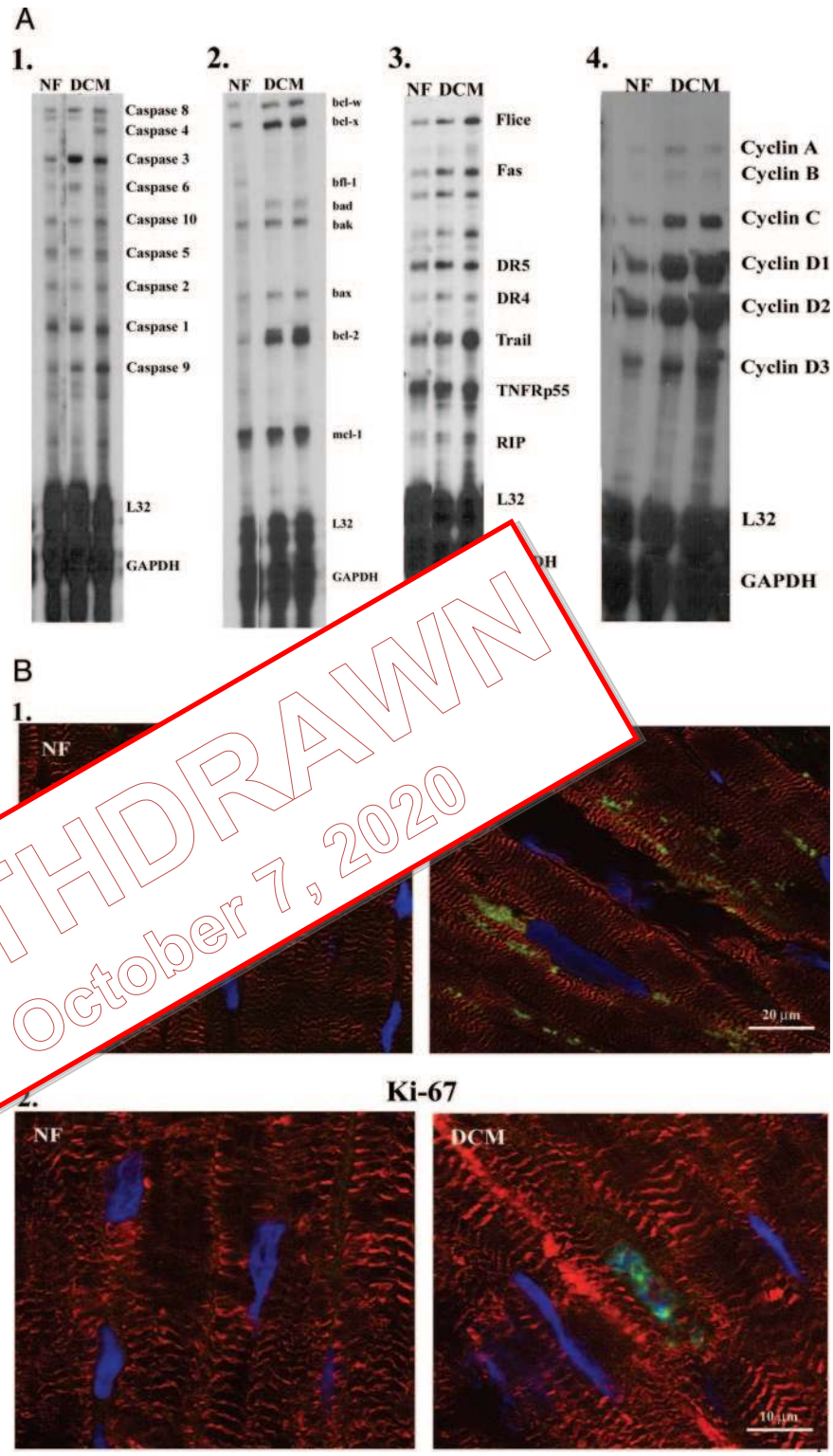

FIG. 9. *A*, changes in expression of apoptotic and cyclin genes in DCM *versus* nonfailing human hearts. Gene expression was analyzed using RPA multiprobes hAPO-1c (*panel 1*), hAPO-2c (*panel 2*), hAPO-3 (*panel 3*), and hCYC-1 (*panel 4*), hybridized to RNA samples of five NF and five DCM human heart samples. Maximum up-regulation of *FAS*, *FADD*, *TRAIL*, *TNFRp55*, *Bcl2*, *BAX*, caspase-3 and -9 was observed in DCM hearts compared with NF samples. The figure is representative of five individual experiments. *B*, expression of active caspase 3 protein and presence of Ki-67 in DCM and nonfailing heart sections. *Panel 1* shows triple staining for α-actinin (*red*), active caspase 3 (*green*), and DAPI (*blue*). Some of the myocytes in DCM sections in the scanned area showed expression of caspase 3 protein. None of the myocytes in NF heart sections showed expression for caspase 3 antibody. *Panel 2* shows ple staining for α-actinin (*red*) (*green*), and DAPI (*blue*). Som clei in DCM cardiomyocyt for Ki-67 immunoreactiv of the myocytes in NF stained positive for the K Magnification is the same a of *B*.

protein was not altered. The enhanced expression of the anti-apoptotic gene in failing hearts, as the authors suggested, was because of compensatory activation mechanisms in overloaded myocardium attempting to maintain cell survival. Ikeda *et al.* (17) reported no change in the expression of either Bax or Bcl2 proteins between the stages of hypertrophy and failure in spontaneously hypertensive rats. Induction of Bax, but not Bcl2, was observed during the transition to left ventricular dysfunction during chronic pressure overload in rats (11). Our study in 9-month-old Tg mice overexpressing myotrophin showed a significant increase in both the pro-apoptotic gene *Bax*, as well as the anti-apoptotic gene *Bcl2*, at both RNA and protein levels during transition from hypertrophy to heart failure. Levels of Bcl-xl and Bfl-1 transcripts were also elevated in the failing heart (Fig. 2). Considerable increases in Cd13 and Cd14 macrophages were also observed in failing hearts, suggesting that the dying cells are ingested by infiltrating macrophages in the failing myocardium (Fig. 4*C*).

Like apoptosis, cell division is a fundamental and ubiquitous process in multicellular organisms. The molecules that regulate cell cycle progression, cyclins and Cdks (18, 19), are well characterized. The kinase activity of Cdks is dependent on the

presence of activating subunits, the cyclins. Evidence exists to suggest that apoptosis and the cell cycle may be interconnected (20). For example, expression of the proto-oncogene c-*myc* stimulates cell proliferation and can also predispose cells to apoptosis when growth factors are limiting (16). Recent work now indicates that the apoptotic regulatory proteins themselves can directly impinge on the cell cycle machinery (21, 22). Thus as a cell progresses through the cell cycle, it must determine whether to complete cell division, arrest growth to repair cellular damage, or undergo apoptosis if the damage is too severe or if the cell is incapable of repairing the DNA. Our data show significant up-regulation of different cyclin genes (*A2*, *B1*, *B2*, *D1*, and *D2*) in failing hearts compared with the age-matched WT hearts, at the transcription and translation levels. Some increase in these proteins in 4-week-old Tg mice compared with age-matched WT mice seems logical, given the need for growth during this period. We also observed significant induction of Cdk activity in hearts from 9-month-old Tg mice. Cdk1 and Cdk2 were induced more than 4-fold in failing hearts compared with nonfailing hearts (Fig. 6*D*). So the question remains, why is remodeling needed, especially at the end stage? We postulate that, after longstanding hypertrophy, the myocardial response to compensate for cell loss causes more cardiac cells to reenter the cell cycle. Our results suggest that c-*myc* and cyclins are involved at an important nodal point shared by pathways regulating cellular proliferation and apoptosis. It is possible that protection against cell death by Bcl2 indirectly augments the induction of multiple cyclins and Cdks.

In this study, we have documented significant c
several cell cycle regulatory proteins and regulat
failing hearts. The expression of pCNA, proli
nuclear antigen Ki-67, has been demon
undergoing severe stress (23). P
histone H3 is tightly correlate
during both mitosis and
presence of the Ki-67
hearts (Fig. 8*A*). Brom
out of 3893 ± 423 cell
myocytes of failing heart
phohistone H3 (Ser-10), pC
detected
in much higher amounts
myocytes of
9-month-old Tg mice, compare
ytes from nonfailing
(WT and 4-week-Tg) heart sa
(Fig. 8*B*). More importantly, colocalization of overexpressed cyclin and phosphohistone H3 was observed in myocytes from failing myocardial sections of Tg mice (Fig. 8*C*). Significant up-regulation of these cell cycle marker proteins in myocytes of 9-month-old Tg hearts convincingly points toward a regeneration process in failing hearts and specifically provides evidence of proliferation of cardiac myocytes in response to stress. Although one can argue that the up-regulation of cell regeneration markers may be because of nuclear division in myocytes, as myocytes are known to be multinucleated. However, we have always compared our data to age matched WT mice where no evidence of such cell regeneration was observed. Our data thus suggest, for the first time, that both cell death (Fig. 7) and cell regeneration (Fig. 8) occur in the myocytes (although the frequency is small, ~0.08%) during the transition from hypertrophy to heart failure, although the origin of cycling myocytes in heart failure is an interesting and yet unsolved and debatable issue. To validate our data that myocytes do undergo simultaneous apoptosis and cell regeneration during heart failure in Tg mice hearts, we have compared the gene profiles of several apoptotic and cell cycle regulator genes in DCM human hearts, compared with nonfailing ones. The transcript profiles of several apoptotic as well as cell cycle regulator genes have shown similar changes between DCM hearts and murine heart failure model overexpressing myotrophin. We have also shown up-regulation of active caspase 3 protein and Ki-67 positive nuclei in myocytes of DCM heart samples (Fig. 9*B*). Dividing myocytes may also originate from cardiac stem cells or from migratory stem cells. As reported by Beltrami *et al.* (25) stem cells may regenerate myocytes that have been lost by severe stress, then go into "overdrive" in response to significant myocyte loss. Myocyte proliferation may be a component of the growth reserve of the heart upon demand, and there is evidence that regeneration in myocytes may challenge the dogma that the heart is a post-mitotic organ (6, 23). Furthermore, the ability of the heart to replace damaged myocardium and induce cell division during failure suggests that there is a continuous turnover of cells during the lifespan of the organism. Because the heart ultimately goes to failure, it can be postulated that under severe stress, the cell death process ultimately overtakes the regeneration machinery in the defective myocardium during heart failure. Apoptosis and cell regeneration thus can be because of a combined effect of neurohumoral changes and mechanical factors in addition to inc cardiac mass, which triggers the heart to go to fa everely compromised cardiac function. Studies xplore the frequency of cell death in cel ac myocytes. Because our data sh eneration do not occur du onset of the disease), it recise time point at egeneration process phy to heart failure in are model. This information ine the optimal time to start deadly disease.

—We thankfully acknowledge the heart transplant Moravec and Wendy Sweet (Transplant Tissue Core), the human hearts.

REFERENCES

1. Cheng, W., Li, B., Kajstura, J., Li, P., Wolin, M. S., Sonnenblick, E. H., Hintze, T. H., Olivetti, G., and Anversa, P. (1995) *J. Clin. Investig.* **96,** 2247–2259
2. Edwards, D. R. (1994) *Trends Pharmacol. Sci.* **15,** 239–244
3. Kajstura, J., Cheng, W., Sarangarajan, R., Li, P., Li, B., Nitahara, J. A., Chapnick, S., Reiss, K., Olivetti, G., and Anversa, P. (1996) *Am. J. Physiol.* **271,** H1215–H1228
4. Kajstura, J., Cheng, W., Reiss, K., Clark, W. A., Sonnenblick, E. H., Krajewski, S., Reed, J. C., Olivetti, G., and Anversa, P. (1996) *Lab. Investig.* **74,** 86–107
5. Olivetti, G., Abbi, R., Quaini, F., Kajstura, J., Cheng, W., Nitahara, J. A., Quaini, E., Di Loreto, C., Beltrami, C. A., Krajewski, S., Reed, J. C., and Anversa, P. (1997) *N. Engl. J. Med.* **336,** 1131–1141
6. Beltrami, A. P., Urbanek, K., Kajstura, J., Yan, S. M., Finato, N., Bussani, R., Nadal-Ginard, B., Silvestri, F., Leri, A., Beltrami, C. A., and Anversa, P. (2001) *N. Engl. J. Med.* **344,** 1750–1757
7. Sen, S., Kundu, G., Mekhail, N., Castel, J., Misono, K., and Healy, B. (1990) *J. Biol. Chem.* **265,** 16635–16643
8. Mitra, S., Timor, A., Gupta, S., Wang, Q., and Sen, S. (2001) *Cytogenet. Cell Genet.* **93,** 151–152
9. Sarkar, S., Leaman, D. W., Gupta, S., Sil, P., Young, D., Morerhead, A., Mukherjee, D., Ratliff, N., Sun, Y, Rayborn, M., Hollyfield, J., and Sen, S. (2004) *J. Biol. Chem.* **279,** 20422–20434
10. Li, Z., Bing, O. H., Long, X., Robinson, K. G., and Lakatta, E. G. (1997) *Am. J. Physiol.* **272,** H2313–H2319
11. Condorelli, G., Morisco, C., Stassi, G., Notte, A., Farina, F., Sgaramella, G., de Rienzo, A., Roncarati, R., Trimarco, B., and Lembo, G. (1999) *Circulation* **99,** 3071–3078
12. Casciola-Rosen, L., Nicholson, D. W., Chong, T., Rowan, K. R., Thornberry, N. A., Miller, D. K., and Rosen, A. (1996) *J. Exp. Med.* **183,** 1957–1964
13. Black, S. C., Huang, J. Q., Rezaiefar, P., Radinovic, S., Eberhart, A., Nicholson, D. W., and Rodger, I. W. (1998) *J. Mol. Cell Cardiol.* **30,** 733–742
14. Hockenbery, D. M., Oltvai, Z. N., Yin, X. M., Milliman, C. L., and Korsmeyer, S. J. (1993) *Cell* **75,** 241–251
15. Yonish-Rouach, E., Resnitzky, D., Lotem, J., Sachs, L., Kimchi, A., and Oren, M. (1991) *Nature* **352,** 345–347
16. Evan, G. I., Wyllie, A. H., Gilbert, C. S., Littlewood, T. D., Land, H., Brooks, M., Waters, C. M., Penn, L. Z., and Hancock, D. C. (1992) *Cell* **69,** 119–128
17. Ikeda, S., Hamada, M., and Hiwada, K. (1999) *Clin. Sci. (Lond.)* **97,** 239–246
18. Norbury, C., and Nurse, P. (1992) *Annu. Rev. Biochem.* **61,** 441–470
19. Morgan, D. O. (1995) *Nature* **374,** 131–134
20. Meikrantz, W., and Schlegel, R. (1995) *J. Cell. Biochem.* **58,** 160–174
21. Brady, H. J., Gil-Gomez, G., Kirberg, J., and Berns, A. J. (1996) *EMBO J.* **15,** 6991–7001

22. Mazel, S., Burtrum, D., and Petrie, H. T. (1996) *J. Exp. Med.* **183,** 2219–2226
23. Zorc, M., Vraspir-Porenta, O., Zorc-Pleskovic, R., Radovanovic, N., and Petrovic, D. (2003) *Cardiovasc. Pathol.* **12,** 36–39
24. Hendzel, M. J., Wei, Y., Mancini, M. A., Van Hooser, A., Ranalli, T., Brinkley, B. R., Bazett-Jones, D. P., and Allis, C. D. (1997) *Chromosoma* (*Berl.*) **106,** 348–360
25. Beltrami, A. P., Barlucchi, L., Torella, D., Baker, M., Limana, F., Chimenti, S., Kasahara, H., Rota, M., Musso, E., Urbanek, K., Leri, A., Kajstura, J., Nadal-Ginard, B., and Anversa, P. (2003) *Cell* **114,** 763–776
26. Scarabelli, T. M., Stephanou, A., Pasini, E., Comini, L., Raddino, R., Knight, R. A., and Latchman, D. S. (2002) *Circ. Res.* **90,** 745–748
27. Reiss, K., Cheng, W., Giordano, A., De Luca, A., Li, B., Kajstura, J., and Anversa, P. (1996) *Exp. Cell Res.* **225,** 44–54
28. Sil, P., Kandaswamy, V., and Sen, S. (1998) *Circ. Res.* **82,** 1173–1188
29. United States National Institutes of Health (1996) *Guide for the Care and Use of Laboratory Animals*, NIH Publication 85-23, National Institutes of Health, Bethesda, MD